International Journal of Computer Information Systems and Industrial Management Applications.
ISSN 2150-7988 Volume 15 (2023) pp. 238-249

Received: 19 Jan. 2023; Accepted: 27 May, 2023; Published: 9 June, 2023

Automatic Skin Lesion Segmentation using a Hybrid Deep Learning Network

Ranjita Rout[1], Priyadarsan Parida[2] and Sonali Dash[3]

[1,2] Department of Electronics and Communication Engineering,
GIET University, Gunupur, Rayagada, Odisha, India
ranjitarout@gietl.edu
priyadarsanparida@giet.edu

[3] Department of Computer Science Engineering,
Chandigarh University, Chandigarh, Punjab, India
sonali.isan@gmail.com

***Abstract*: Skin cancer occurs due to the abnormal development of the skin cells. It is extremely important to identify this change in skin cells as soon as possible otherwise it is harmful to human life. Among all, malignant melanoma or melanoma is a more dangerous skin cancer. The automatic and accurate identification of melanoma is highly essential as it helps in the diagnosis process. The proposed model uses the Histogram Equalization (HE) and Adaptive gamma correction with weighting distribution (AGCWD) techniques for enhancement of the texture region to obtain better segmentation results. Further, the proposed model focuses to detect the skin lesion automatically by combining DeepLabV3+ with the different base networks such as ResNet 18, ResNet 50 and MobileNetV2. The proposed model is tested using a variety of images from the ISIC 2016, ISIC 2017 and ISIC 2018 datasets. The proposed model is evaluated by comparing with the existing approaches.**

***Keywords*:** DeepLabV3+**,** Pre-processing, Dermoscopic images, Histogram Equalization, AGCWD, Skin lesion**.**

I. Introduction

In the recent years, skin cancer becomes a common disease [1]. It is mainly divided into three categories known as squamous cell carcinoma, basal cell carcinoma and melanoma. Among all, melanoma is considered as most fatal skin cancer. It is curable if detected early and with proper diagnosis. Primarily, the visual inspection helps the dermatologists to identify melanoma. During the visual examination, ABCDE [2] rule is used by the dermatologists. But sometimes the visual examination fails to provide the precise result due to the large variation in affected regions such as variation in illumination, intensity in boundary regions etc. So, imaging assisted diagnosis technique is preferred using artificial intelligent techniques. These approaches use image segmentation for extracting skin lesions from healthy skin using dermoscopic images [3]. Furthermore, due to poor contrast in the dermoscopic image it is very difficult to distinguish between healthy skin regions and skin lesion regions. The air bubbles, hairs, black frame, ruler mark, blood vessel etc. are the present additional constraints that make it even harder to segment skin lesions from the dermoscopic images. Figure 1 shows a few samples of dermoscopic images taken from the datasets having variation in color, texture, shape, intensity etc. along with existence of other artifacts.

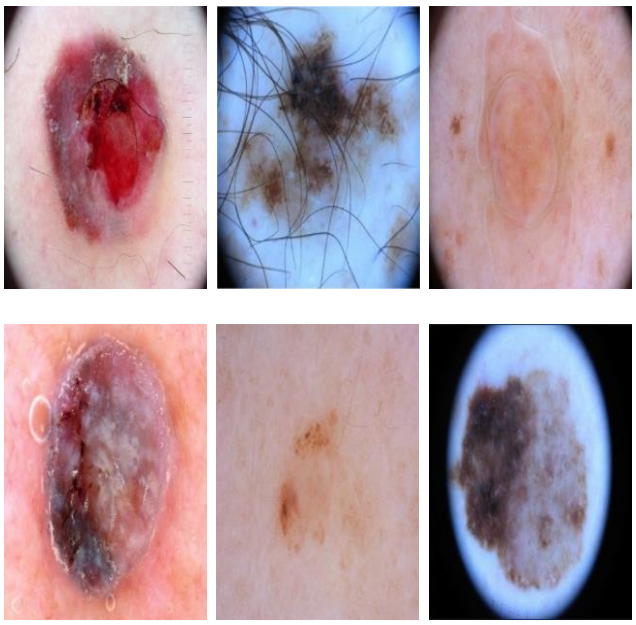

Figure 1. Sample of dermoscopic images available in the datasets.

The presence of the aforementioned unwanted artifacts makes a challenging task during accurate identification of skin lesion. So, it is highly essential to develop the algorithms that helps to automatically detect the melanoma with better accuracy by ignoring the unwanted artifacts. These algorithms not only help the experts for automatic detection of melanoma but also in the proper diagnosis process that leads the survival rate of human life. Preprocessing, segmentation, feature extraction, and classification are the four basic steps used in the automatic melanoma detection [4] and classification process. The preprocessing technique [5] is the

first and fundamental step that helps to remove the presence of the unwanted artifacts from the dermoscopic images. Segmentation technique helps to segregate the skin lesion region from the healthy skin regions. A number of unsupervised and supervised approaches are available for identification of skin lesions. The existing unsupervised approaches such as thresholding [6], clustering [7,8], region based [9,10] etc. are available for lesion segmentation. Among all, thresholding is one of the most popular technique for segmenting skin lesions due to its simplicity. Apart from the unsupervised approaches, the hybrid approaches [10-12] are widely used for its better segmentation results. It can be achieved by combining more than one approaches. Most widely used hybrid approaches for image segmentation are transition region based [13], saliency based [14], active contour [15] etc.

In the present era, supervised approaches based on Convolutional neural networks (CNNs) [16-20] are widely employed for segregating and classifying skin lesions due to its superiority as compared to the traditional and hybrid approaches. Many methods for semantic segmentation are based on CNNs, in which each pixel is labelled with the class of the object or region it surrounds. Deep learning (DL) [21-23] models, in particular convolution neural network (CNN), have recently attracted increased interest in a variety of applications, including object identification, segmentation and classification.

II. Related work

To provide a reliable and accurate identification process, the skin lesion must be separated from the nearby healthy skin regions and key features must be highlighted. Various segmentation methods have been developed by the researchers and discussed in the literature. The traditional skin lesion segmentation approaches such thresholding [6], clustering [7], region based [9,10] are the popularly used segmentation techniques due to its simplicity. Apart from the traditional approaches, the hybrid approaches such as transition region [13], saliency based [11], active contour [15] also developed for identification of skin lesions. A hybrid model is developed by Hwang et al. [24] by combining the k-means with a level set for lesion identification. To improve the contrast of the lesion regions, an Automatic Color Equalization (ACE) technique is used by Schaefer et al. [25] in the proposed model. The ACE technique helps to improve the contrast of the image more accurately in the red channel and provides a better segmentation result.

The conventional skin lesion segmentation techniques that were in use prior to the CNN architecture frequently relied on the manually selection of features. So, in the recent years, researchers are focusing on CNN based approaches for automatic extraction of features to improve the accuracy. A cascaded context augmentation neural network is developed by Wang et al. [26] for automatic segmentation of lesion regions. The cascaded context aggregation (CCA) module is essentially used to successively and selectively combine the input image and multi-level characteristics from the encoder sub-network utilizing a gate-based information integration strategy. For dermoscopic images with corner boundaries of various sizes or borders of colors, provide inadequate skin lesion segmentation results. To overcome this problem, a machine learning-based skin lesion segmentation method is developed by Rehman et al. [27] that can eliminate boundaries with corners of varying sizes and/or colors that are similar to the color of the lesion. To enhance the dermoscopic images, the modified histogram and log exponential transformation is employed and further the GrabCut method is used for segmentation. A mask-R-CNN method is developed by [16] for the effective segmentation of lesion regions. A full-resolution CNN (FrCN) is developed by [28] for the segmentation of skin lesions. Without pre-processing, FrCN can learn attributes from full-resolution lesion photos. You Only Look Once (YOLO) and GrabCut algorithms were integrated by Unver et al. [29] for efficient segmentation. DeepLab V3+ and Mask R-CNN developed by [30] to identify the skin lesion precisely. Lesion segmentation is accomplished by combining the encoder with DeepLabV3 and the decoder [31]. For feature extraction, Khan et al. [32] implemented transfer learning method with a deep CNN. The best characteristics were selected using kurtosis-controlled principle component analysis. The proposed model provides a generic model for skin melanoma identification using CNN and its performance improvement by utilizing dermoscopic image enhancement approaches.

III. Proposed Model

The proposed model is designed to identify the lesion regions automatically from dermoscopic images. It basically combines deep learning architecture with the pretrained networks such as ResNet 18, ResNet50, MobiltNetV2 for identification of skin lesions. The more details about the proposed model is explained in the following subsections.

A. Pre-processing techniques

The images present in the datasets are having large variation in shape, size, illumination etc. Apart from that, it is found that the hairs, gels, ruler marks etc. are also available in the images. The presence of aforementioned artifacts increases the computational time and also provides the incorrect skin lesion identification results. Hence, the pre-processing step is highly essential as it removes the undesired artifacts and helps for further processing and also increases the segmentation accuracy. The preprocessing steps includes the enhancement of texture regions using Histogram Equalization (HE), Adaptive gamma correction with weighting distribution (AGCWD) enhancement technique and removal of undesired artifacts.

B. Enhancement of images using Histogram Equalization (HE)

As enhancement techniques help for enhancing the quality of image as well as for subsequent processing, hence in the recent years it is frequently used in medical imaging. A variety of methods for improving images quality have been developed. Among all, Histogram Equalization (HE) [33] is one the simplest enhancement technique. It uses the histogram of an image to enhance the image in a spatial domain while processing images. The global contrast of the processed image is typically increased by histogram equalization. The algorithm of the HE is as follows;

i. Take the original image.

ii. Calculate the histogram of the image.
iii. Define the local minima of the image.
iv. Based on the local minima, split the histogram.
v. Each histogram split should contain the precise grey levels.
vi. Employ the HE to each split.

The enhanced image obtained after HE is illustrated in Figure 2. The original images are illustrated in Figure 2(a). Based on the visual analysis, it is found that due to color variation in lesion regions and healthy skin regions it is quite challenging to identify the accurate lesion regions. Hence, HE algorithm is employed to enhance the texture regions so that it helps to retrieve the features of lesion regions using the pretrained networks to provide a better segmentation result.

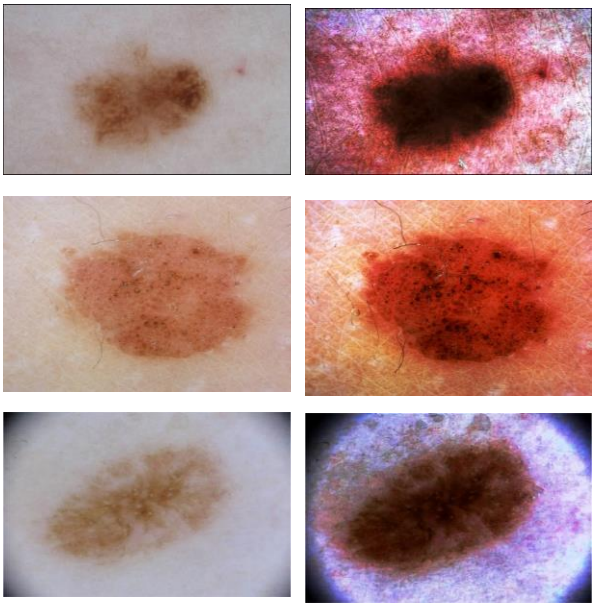

(a) (b)

Figure 2. Histogram Equalization output (a) original image, (b) enhanced image after HE.

C. Enhancement of images using Adaptive Gamma Correction Weighted Distribution (AGCWD)

A hybrid function for histogram modification is adaptive gamma correction with weighting distribution (AGCWD) [34]. It basically combines conventional gamma correction and histogram equalization for improving the contrast of the image. By utilizing the smoothing curve in gamma correction, the contrast of the image can be automatically improved [35]. When the input image doesn't have enough bright pixels, this technique might not yield the desired results because the highest intensity in the output image is bound by the highest brightness of the input image [36]. The output obtained after AGCWD technique is displayed in Figure 3. Figure 3(a) displays the original image and the enhanced image obtained after AGCWD technique is illustrated in Figure 3(b).

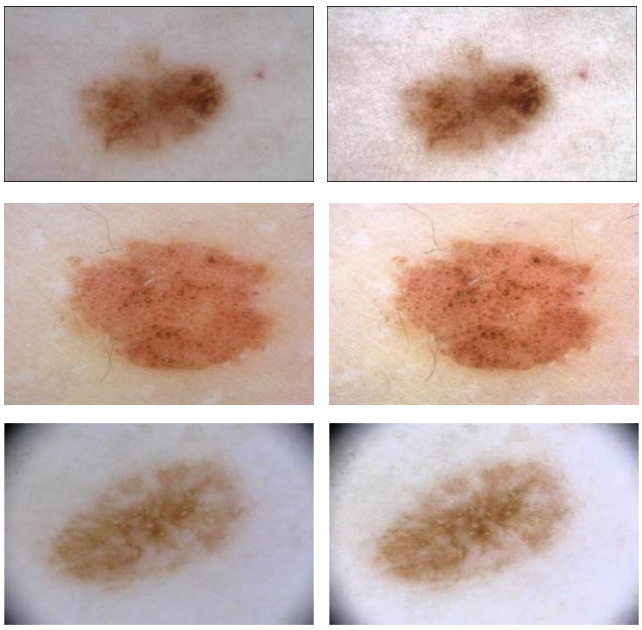

(a) (b)

Figure 3. AGCWD output (a) original image, (b) enhanced image after AGCWD.

D. Removal of undesired artifacts

The proposed model uses the DullRazor [37], a well-known hair-removal technique to eliminate undesired artifacts from the images. After enhancement technique (HE or AGCWD), the hair removal technique is implemented to eliminate the artifacts. Further, the inpainting technique is employed to replace the hair masks with the neighbourhood healthy pixel regions. The output obtained after hair removal technique is illustrated in the Figure 4. The original image is illustrated in Figure 4(a). The enhanced images after HE and their corresponding output images obtained after removal of artifacts are illustrated in Figure 4(b) and Figure 4(c). The AGCWD enhanced images and the output obtained after hair removal technique is shown in Figure 4(c) and Figure 4(d). From the visual analysis, it is found that after enhancement, the lesion regions are more prominent than the original images. So, it becomes more easier to separate the lesion regions. But after hair removal of enhanced image, the resultant image becomes more blurred as compared to the enhanced image. Hence, it is a challenging task to identify the accurate lesion regions.

E. Automatic skin lesion identification by combining the DeepLabV3+ with pretrained networks

The proposed model combines the pretrained networks i.e. ResNet 18, ResNet50 and MobileNetV2 with the DeepLabV3+ for accurate identification of lesion regions from dermoscopic images. The features of the dermoscopic images are extracted using the pretrained network and applied as an input to the DeepLabV3+ network for further processing. Atrous spatial pyramid pooling has been improved with the inclusion of image-level features and batch normalization in DeepLabv3 [38]. The last few backbone blocks contain atrous convolutional to regulate the size of the feature map. On top of taken features that categorize each pixel in accordance with their classifications, the impressive spatial pyramid pooling is applied. The enhanced images obtained after HE and AGCWD techniques are applied to each model for

identification of skin lesions. The features from the enhanced images are retrieved using the pretrained networks and applied as an input to the DeepLabV3+ for automatic identification of lesion regions. In order to lower the loss with the least amount of effort, an optimizer is crucial in changing the various model parameters. The proposed model utilizes adaptive moment estimation (ADAM) optimizer for all of the experimental work because it offers a quick loss function reduction for all datasets compared to the conventional stochastic gradient descent momentum (SGDM) algorithm. Figures 5 and 6 represents the architecture of the proposed model. Figure 5 displays the architecture of the proposed model without using hair removal technique. The enhanced images obtained after HE and AGCWD techniques are applied as input to the base network for extraction of features. As the number of artifacts are present in the enhanced images, hence to remove the artifacts from the enhanced images, the popularly used DullRazor algorithm is employed. The output obtained after the removal of artifacts is further applied as inputs to the proposed model. The architecture is illustrated in Figure 6.

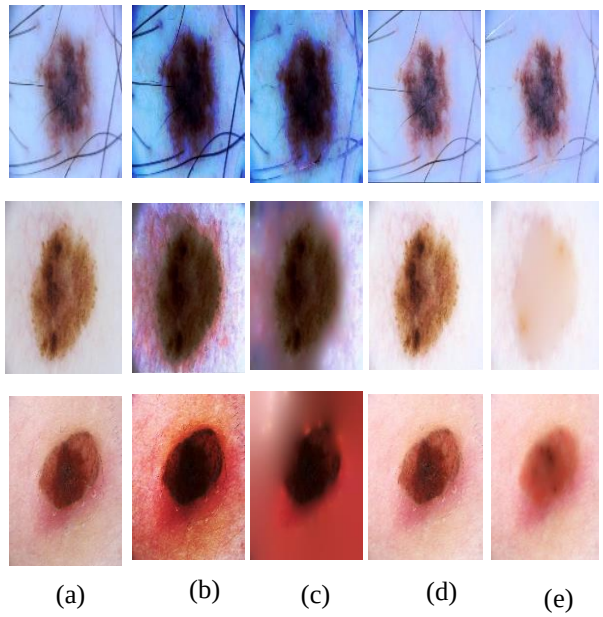

Figure 4. (a)Original image;(b) HE enhanced image; (c)output obtained after hair removal of (b); (c) AGCWD enhanced image, (d) output obtained after hair removal of (c).

The dermoscopic images from three datasets such as ISIC 2016, ISIC 2017 and ISIC 2018 are considered to assess the performance of the proposed model. The algorithm of the proposed model is outline as;

Step-1: Consider the input images from the dataset.
Step-2: Enhance the images using HE/AGCWD algorithm.
Step-3: Create an image datastore by taking the enhanced images.
Step-4: Specify the various classes.
Step-5: Use the ground truth images to generate a pixel label image datastore.
Step-6: Resize the enhanced images as per the input size of the base network.
Step-7: Develop a pixel label image datastore for the resized images.
Step-8: Divide the dataset for training and testing randomly.
Step-9: Specify the different training parameters of the network.
Step-10: Train the Network based on the parameters specified in step 9.
Step-11: Consider the images randomly to test the network.
Step-12: Calculate the performance measure parameters to determine the performance of the network.

IV. Datasets used

The dermoscopic images from ISIC2016 [39], ISIC 2017 [40] and ISIC 2018 [41] datasets are utilized in the proposed model. The images of various sizes, shapes, and resolutions are available in the datasets. The datasets contain both the original images and the ground truths. The ground truths are compared with the lesion masks extracted from the proposed model to evaluate the performance measures. The maximum size of RGB image is of 6748×4499. The RGB images are resized as per the input size of the pretrained network to decrease the computational time.

V. Performance measures

The proposed model is evaluated by using the different performance measures i.e. Accuracy (Acc), Jaccard Index (JI), Dice Coefficients (DC). Since the datasets included the ground truths, they were compared to the lesion mask produced by the proposed model to calculate the performance measures. The true positive, true negative, false positive and false negative rates are represented as TP, TN, FP, and FN in a confusion matrix that was created by considering the ground truth and the lesion mask got from the proposed model. The various metrics are represented as;

$$Accuracy = \frac{TP + TN}{TP + FP + TN + FN} \tag{1}$$

$$JI = \frac{TP}{(TP + FP + FN)} \tag{2}$$

$$DC = \frac{2 \times TP}{(TP + FP) + (TP + FN)} \tag{3}$$

The values for the different metrics are varies from 0 to 1 where 0 represents the worst value and 1 represents the best value.

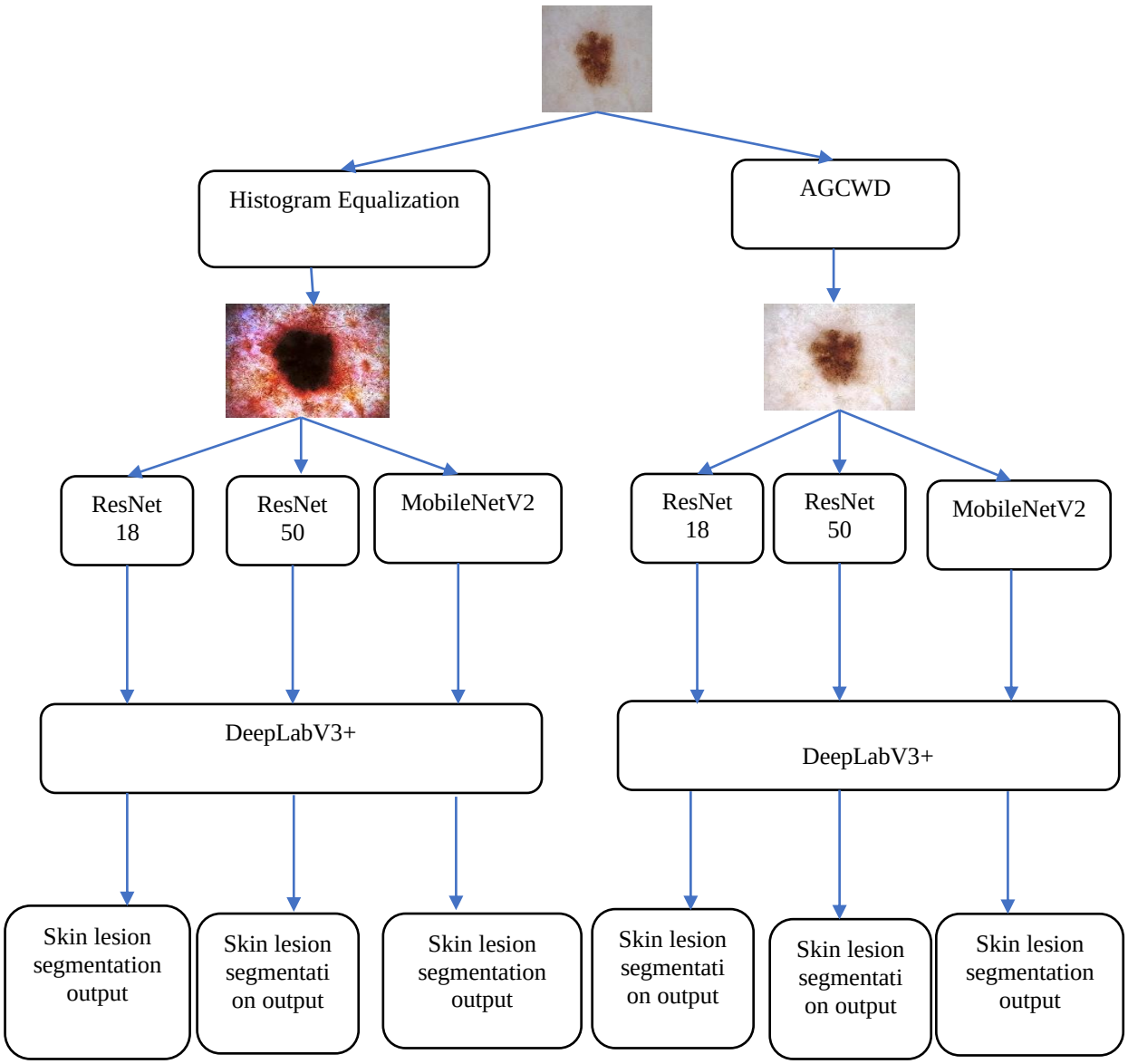

Figure 5. Architecture of the proposed model without hair removal technique.

VI. Results and Discussion

MATLAB 2017a was used to conduct the complete experiment on a computer with a Core i3 processor. The proposed model is evaluated using a wide range of images from the datasets. Initially, the proposed model is tested by using the enhanced images (HE and AGCED) without hair removal technique. The enhanced images are applied as input to the different pretrained networks such ResNet 18, ResNet 50 and MobileNetV2 for extraction of features. The extracted features applied as input to the DeepLabV3+ for automatic identification of lesion regions. Further, the proposed model is tested by considering the enhanced images along with hair removal technique. The quantitative measures obtained using enhanced images without hair removal and with hair removal technique for ISIC 2016 dataset is given in Table 1.

Table 1 demonstrates that the proposed model yields the best segmentation results for the ResNet 18 using the HE enhanced images as compared to the AGCWD enhanced images. But the other combinations of the proposed model also achieve comparable good results compared to the existing approaches. For qualitative analysis, the results obtained from the proposed model for ResNet 18 using ISIC 2016 dataset is illustrated in Figure 7. The original images from the dataset are shown in Figure 7(a). The enhanced images after HE is illustrated in Figure 7(b) and the predicted skin lesions obtained from the proposed model is demonstrated in Figure 7(c).

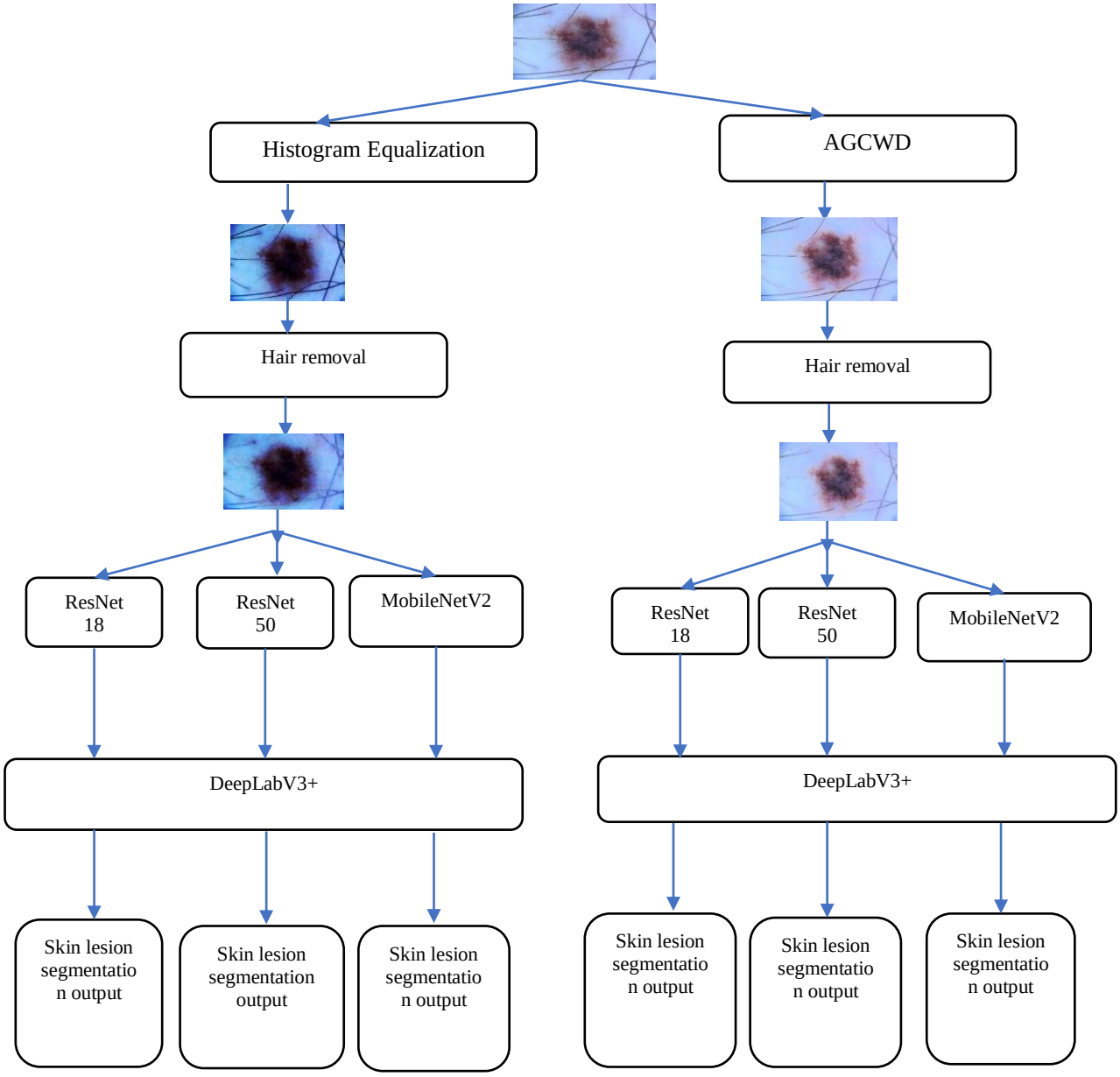

Figure 6. Architecture of the proposed model with hair removal technique.

Table 1. Experimental results from the proposed model using ISIC 2016.

Year	Method	Accuracy (%)	JI (%)	DC (%)
2018	DRN [42]	86.1	---	---
2018	NDB [43]	83.2	---	---
2016	Sparse coding [44]	91.0	67.0	91.0
2019	FCHM [45]	93.4	79.1	86.9
2017	DCN [46]	92.3	80.6	89.2
2019	KSRBM[47]	93.0	83.6	91.2
2008	SRM [48]	91.0	67.0	80.0
2016	SLMSSP [49]	85.68	66.19	75.88
2017	SBLS [50]	84.67	57.20	69.97
2022	CCEN [26]	----	87.1	----
Proposed Model	ResNet 18 + HE	**94.75**	**90.07**	**91.86**
	ResNet 50 + HE	93.36	89.9	91.02
	MobileNetV2 + HE	91.90	88.54	89.08
	ResNet 18 + HE + Hair removal	92.07	89.74	90.24
	ResNet 50 + HE + Hair removal	91.23	85.91	89.37
	MobileNetV2 + HE + Hair removal	89.56	85.34	88.32
	ResNet 18 + AGCWD	93.06	88.61	91.23
	ResNet 50 + AGCWD	92.09	87.06	89.99
	MobileNetV2 + AGCWD	92.05	88.96	87.45
	ResNet 18 + AGCWD + Hair removal	91.24	88.09	89.30
	ResNet 50 + AGCWD + Hair removal	90.31	89.89	90.87
	MobileNetV2 + AGCWD +Hair removal	91.32	88.96	87.45

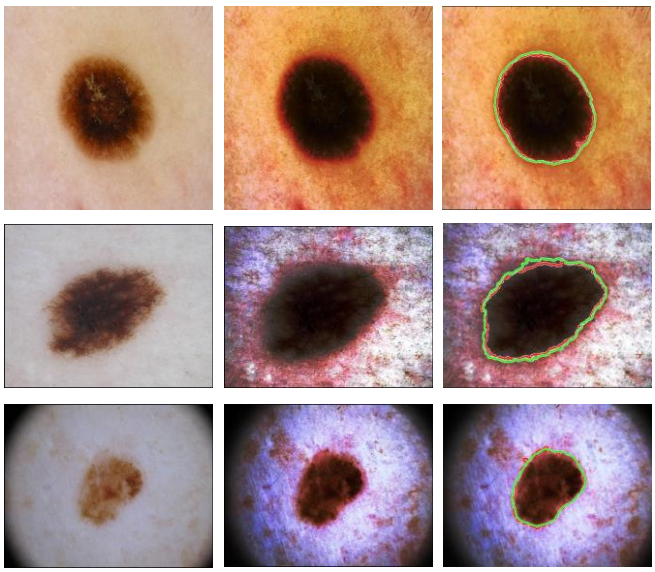

(a) (b) (c)

Figure 7. Results obtained using ISIC 2016 dataset; (a) Original, (b) enhanced image using HE, (c) Extracted lesion from proposed model.

The results obtained using ResNet 18 for AGCWD enhanced images is illustrated in Figure 8. Figure 8(a) and Figure 8(b) display the original images and the associated enhanced images. The predicted lesion regions identified from the proposed model for ISIC 2016 dataset is demonstrated in Figure 8(c).

In Figure 7(c) Figure 8(c), the green color represents predicted lesion regions whereas the actual lesion regions are highlighted in red color. After analyzing the results shown in Figure 7(c) and Figure 8(c), it is found that ResNet 18 performs well for HE enhanced images as compared to AGCWD as the predicted lesions are closer to the actual lesion regions which is shown in Figure 7(c).

Further, the proposed model is evaluated by considering the images from ISIC 2017 dataset. Images of various types are considered and the texture regions are enhanced using HE and AGCWD. The enhanced images without hair removal technique are applied as input to the base networks. The enhanced images applying with hair removal technique are also applied as input to the pretrained networks. The performance measures obtained for different pretrained networks i.e. ResNet 18, ResNet 50 and MobileNetV2 for the quantitative analysis is given in Table 2.

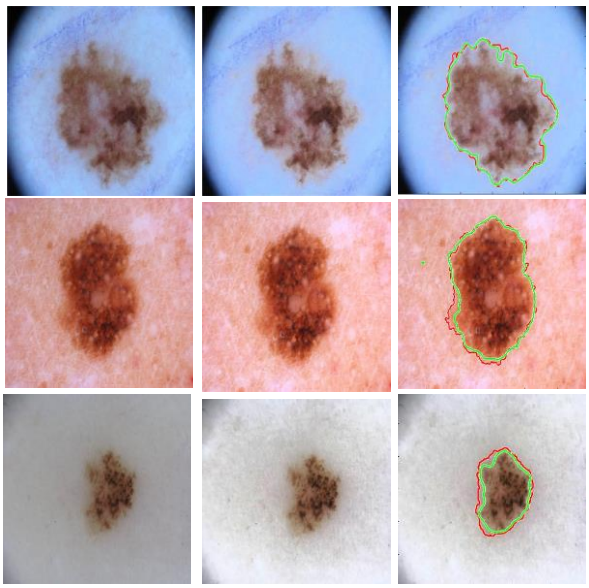

(a) (b) (c)

Figure 8. Results obtained using ISIC 2016 dataset; (a) Original, (b) enhanced image using AGCWD, (c) Extracted lesion from proposed model.

Table 2. Experimental results from the proposed model using ISIC 2017.

Year	Method	Accuracy (%)	JI (%)	DC (%)
2022	FCN-ResAlexNet [51]	93.47	77.54	87.35
2022	SAN [52]	93.43	76.92	85.23
2019	FCN [53]	93.0	75.2	83.7
2020	SegNet [17]	91.76	69.63	82.09
2021	ASCU-Net [54]	92.6	74.2	----
2019	FocusNet [55]	92.14	75.62	83.15
2019	U-net [56]	93.00	75.20	84.00
2022	CCEN [26]	-----	80.3	----
Proposed Model	ResNet 18+ HE	93.67	88.67	89.76
	ResNet 50+ HE	**94.25**	**90.86**	**90.98**
	MobileNetV2+ HE	93.49	89.59	90.45
	ResNet 18+ HE+ Hair removal	91.83	89.32	88.65
	ResNet 50+ HE+ Hair removal	92.03	85.21	88.54
	MobileNetV2+ HE+ Hair removal	91.78	90.16	90.07
	ResNet 18+ AGCWD	93.94	88.73	90.82
	ResNet 50+ AGCWD	94.59	89.03	90.37
	MobileNetV2+ AGCWD	93.58	87.02	88.40
	ResNet 18+ AGCWD+ Hair removal	91.81	87.31	89.46
	ResNet 50+ AGCWD+ Hair removal	92.07	90.25	90.28
	MobileNetV2+ AGCWD+ Hair removal	92.4	86.97	89.81

Table 2 demonstrates that the proposed model outperforms for ResNet 50 with HE enhanced images with Accuracy of 94.25%. The performance measures obtained for other combinations are also given in Table 2 that represents the results are comparable good in comparison with the existing approaches. The simulation results obtained for ResNet 50 using HE and AGCWD enhanced images is illustrated in Figure 9 and Figure 10. The original images are displayed in Figure 9 (a) and Figure 10(a). The enhanced images are illustrated in Figure 9 (b) and Figure 10(b). The predicted lesions obtained from ResNet 50 for the HE and AGCWD enhanced images is illustrated in Figure 9(c) and Figure 10(c). The red and green colors represent the actual and predicted lesion regions.

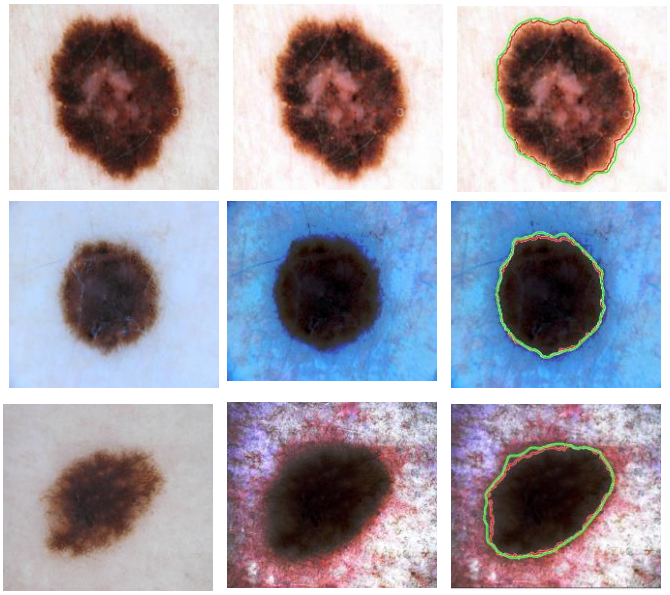

(a) (b) (c)

Figure 9. Results obtained from ResNet50;(a) Original image;(b) HE enhanced image;(c) extracted skin lesion.

The proposed model provides the highest Accuracy of 94.98% for MobileNetV2 for HE enhanced images as compared to the other combinations. The results achieved for other combinations are also given in Table 3. It is observed from the Table 3, the other combinations are also able to provide the good results which are closer to the existing approaches. For qualitative analysis, the simulation results obtained is shown in Figure 11 and Figure 12 for HE and AGCWD enhanced images. The original images considered from ISIC 2018 dataset is illustrated in Figure 11(a) and Figure 12 (a). The enhanced images obtained after HE and AGCWD techniques are displayed in Figure 11(b) and Figure 12(b). The results obtained from the proposed model are illustrated in Figure 11(c) and Figure 12(c). The predicted lesion regions are highlighted in green color whereas the actual regions are predicted in red color. It is evident from the outcomes produced by the proposed model is that it is able to identify the skin lesion regions accurately which is closer to the actual lesion regions [61][62].

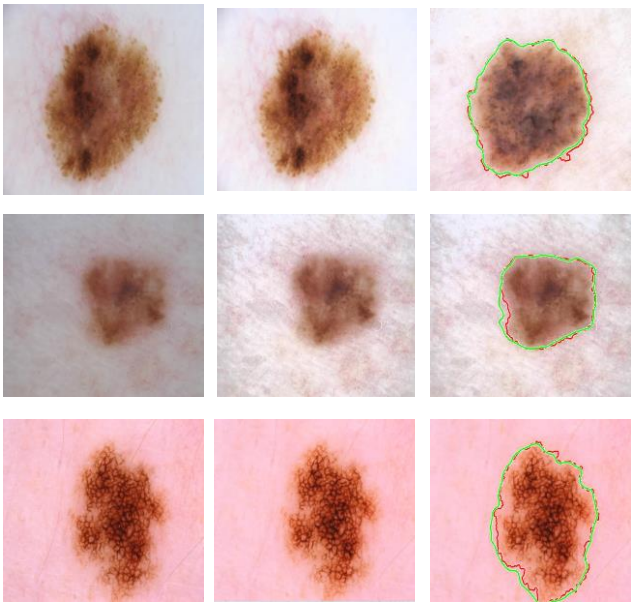

(a) (b) (c)

Figure 10. Results obtained from ResNet50;(a) Original image;(b) AGCWD enhanced image;(c) extracted skin lesion.

Finally, the proposed model is evaluated by considering the images from ISIC 2018 dataset. The enhanced images without hair removal and with hair removal technique are applied as inputs to the pretrained networks. For quantitative analysis, different performance measures are evaluated and given in Table 3.

Table 3. Experimental results from the proposed model using ISIC 2018.

Year	Method	Accuracy (%)	JI (%)	DC (%)
2020	DAGAN [57]	92.9	82.4	88.5
2021	IMF [32]	92.69	---	---
2020	U-Net [58]	---	80.0	87 .0
2019	DCED [59]	---	83.7	90.3
2020	SRMPBMRF [60]	89.47	72.45	80.67
2022	MLBSLS [27]	---	80.0	82.0
Proposed Model	ResNet 18+ HE	92.87	87.89	88.98
	ResNet 50+ HE	93.99	89.85	90.71
	MobileNetV2+ HE	**94.98**	**90.38**	**90.94**
	ResNet 18+ HE + Hair removal	91.36	86.54	87.91
	ResNet 50+ HE + Hair removal	92.79	90.23	89.88
	MobileNetV2+ HE + Hair removal	92.04	91.08	90.36
	ResNet 18+ AGCWD + Hair removal	91.85	88.06	88.51
	ResNet 50+ AGCWD + Hair removal	91.09	90.22	90.04
	MobileNetV2+ AGCWD + Hair removal	92.35	90.14	90.07

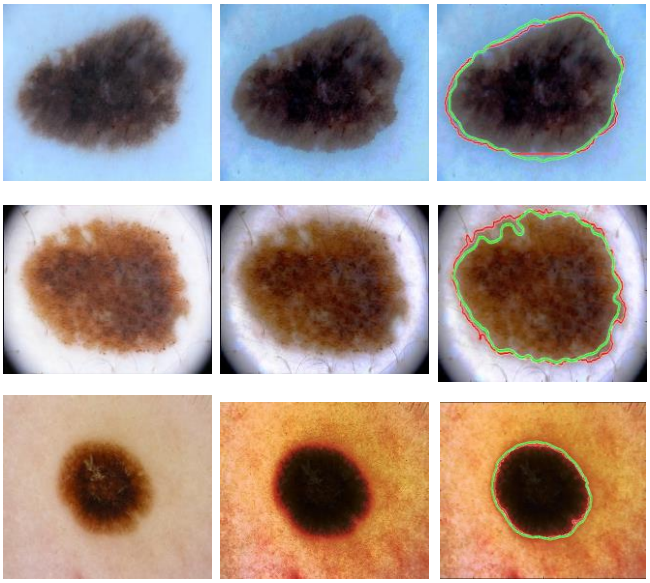

(a) (b) (c)

Figure11. Results obtained from MobileNetV2;(a) Original image;(b) HE enhanced image;(c) extracted skin lesion.

The simulation results obtained after hair removal technique is illustrated in Figure 13. Figure 13 (a) illustrates the original image. The HE enhanced images are shown in Figure 13(b). After hair removal techniques of HE enhanced images, the outputs are displayed in Figure 13(c). The output obtained from the proposed model is illustrated in Figure 13(d) where the red and green colors represents the actual and predicted skin lesion regions. It is observed from the Figure 13(d) that due to the blurring effect after hair removal, it is difficult to predict the accurate lesion regions.

VII. Conclusions

Automatic identification of skin lesions is crucial for the accurate detection of lesion regions. The accurate detection of skin lesion helps the dermatologist in the proper diagnosis process that increases the survival rate. So, the proposed model focuses for automatic identification of skin lesions by combining the different pretrained networks such as ResNet18, ResNet50 and MobileNetV2 with DeepLabV3+. To improve the texture regions, HE and AGCWD enhancement techniques are employed in the proposed model. Along with the enhancement technique, the proposed model uses hair removal technique to remove the undesired artifacts present in the images. In comparison to AGCWD enhanced images, the proposed model accurately detects skin lesions for HE enhanced images and yields improved segmentation outcomes.

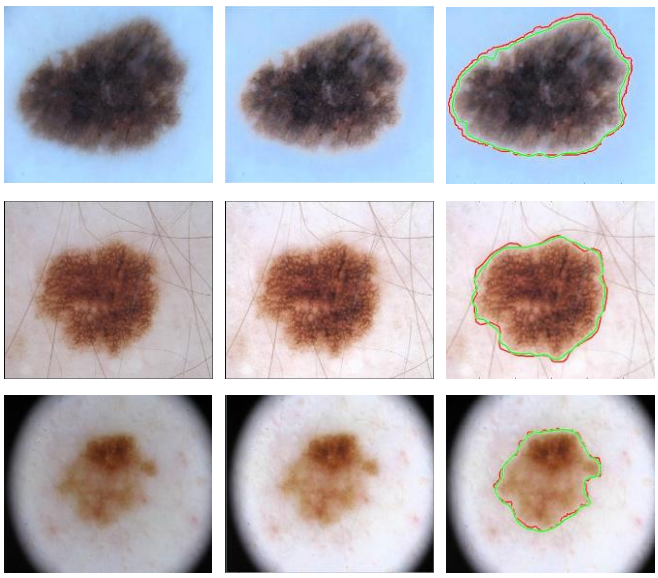

(a) (b) (c)

Figure 12. Results obtained from MobileNetV2;(a) Original image;(b) HE enhanced image;(c) extracted skin lesion.

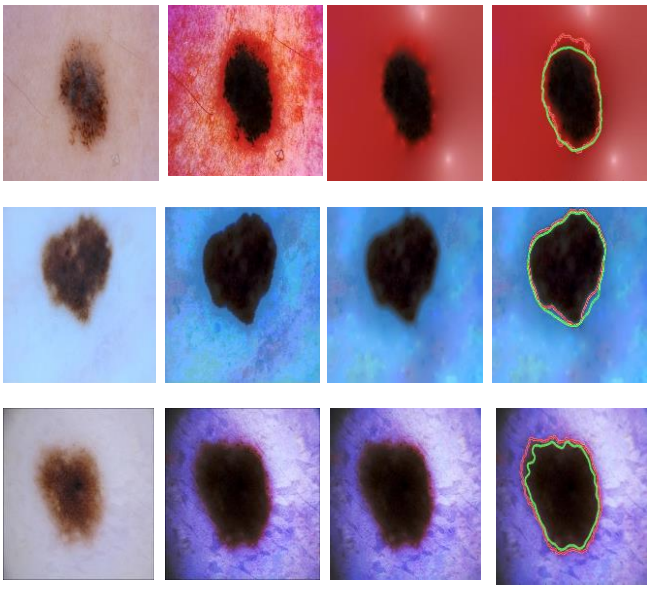

(a) (b) (c) (d)

Figure 13. Results of obtained using ISIC 2016 dataset; (a) Original, (b) enhanced image using HE, (c) hair removal of (b), (d) extracted skin lesion.

Acknowledgment

The authors would thank the authorities of GIET University for extending their support to carry out the research work.

References

[1] Skin Cancer Foundation, 2016, "Skin Cancer Facts & Statistics," SkinCancer.org, 4(1), pp. 1–7.

[2] Daniel Jensen, J., and Elewski, B. E., 2015, "The ABCDEF Rule: Combining the 'ABCDE Rule' and the 'Ugly Duckling Sign' in an Effort to Improve Patient Self-Screening Examinations.," J Clin Aesthet Dermatol, 8(2), p. 15.

[3] Rout, R., Parida, P., and Dash, S., 2023, "A Hybrid Deep Learning Network for Skin Lesion Extraction," pp. 682–689.

[4] [Schmid-Saugeona, P., Guillodb, J., and Thirana, J.-P., 2003, "Towards a Computer-Aided Diagnosis System for Pigmented Skin Lesions," Computerized Medical Imaging and Graphics, 27(1), pp. 65–78.

[5] [Noori, A., Al-jumaily, A., and Noori, A., 2014, "The Beneficial Techniques in Preprocessing Step of Skin Cancer Detection System Comparing," Procedia - Procedia Computer Science, 42(02), pp. 25–31.

[6] Zortea, M., Flores, E., and Scharcanski, J., 2017, "A Simple Weighted Thresholding Method for the Segmentation of Pigmented Skin Lesions in Macroscopic Images," Pattern Recognit, 64, pp. 92–104.

[7] Devi, S. S., Singh, N. H., and Laskar, R. H., 2020, "Fuzzy C-Means Clustering with Histogram Based Cluster Selection for Skin Lesion Segmentation Using Non-Dermoscopic Images," International Journal of Interactive Multimedia and Artificial Intelligence, 6(1), p. 26.

[8] Rout, R., Parida, P., and Patnaik, S., 2021, "Melanocytic Skin Lesion Extraction Using Mean Shift Clustering," *2021 International Conference on Electronic Information Technology and Smart Agriculture (ICEITSA)*, IEEE, pp. 565–574.

[9] Zhou, Y. M., Jiang, S. Y., and Yin, M. L., 2008, "A Region-Based Image Segmentation Method with Mean-Shift Clustering Algorithm," Proceedings - 5th International Conference on Fuzzy Systems and Knowledge Discovery, FSKD 2008, 2, pp. 366–370.

[10] Ali, A.-R., Couceiro, M. S., and Hassenian, A. E., 2014, "Melanoma Detection Using Fuzzy C-Means Clustering Coupled with Mathematical Morphology," *2014 14th International Conference on Hybrid Intelligent Systems*, IEEE, pp. 73–78.

[11] Garnavi, R., Aldeen, M., Celebi, M. E., Varigos, G., and Finch, S., 2011, "Border Detection in Dermoscopy Images Using Hybrid Thresholding on Optimized Color Channels," Computerized Medical Imaging and Graphics, 35(2), pp. 105–115.

[12] Zakeri, A., and Hokmabadi, A., 2018, "ScienceDirect Improvement in the Diagnosis of Melanoma and Dysplastic Lesions by Introducing ABCD-PDT Features and a Hybrid Classifier," Integr Med Res, 38(3), pp. 456–466.

[13] Parida, P., and Rout, R., 2020, "Transition Region Based Approach for Skin Lesion Segmentation," ELCVIA Electronic Letters on Computer Vision and Image Analysis, 19(1), p. 28.

[14] Jahanifar, M., Zamani Tajeddin, N., Mohammadzadeh Asl, B., and Gooya, A., 2019, "Supervised Saliency Map Driven Segmentation of Lesions in Dermoscopic Images," IEEE J Biomed Health Inform, 23(2), pp. 509–518.

[15] Ximenes Vasconcelos, F. F., Medeiros, A. G., Peixoto, S. A., and Rebouças Filho, P. P., 2019, "Automatic Skin Lesions Segmentation Based on a New Morphological Approach via Geodesic Active Contour," Cogn Syst Res, 55, pp. 44–59.

[16] Bagheri, F., Tarokh, M. J., and Ziaratban, M., 2021, "Skin Lesion Segmentation from Dermoscopic Images by Using Mask R-CNN, Retina-Deeplab, and Graph-Based Methods," Biomed Signal Process Control, 67, p. 102533.
[17] Öztürk, Ş., and Özkaya, U., 2020, "Skin Lesion Segmentation with Improved Convolutional Neural Network," J Digit Imaging, 33(4), pp. 958–970.
[18] Bi, L., Kim, J., Ahn, E., Kumar, A., Fulham, M., and Feng, D., 2017, "Dermoscopic Image Segmentation via Multistage Fully Convolutional Networks," IEEE Trans Biomed Eng, 64(9), pp. 2065–2074.
[19] Dash, S., Parida, P., and Mohanty, J. R., 2023, "Illumination Robust Deep Convolutional Neural Network for Medical Image Classification," Soft comput.
[20] Mohanty, A. S., Parida, P., and Patra, K. C., 2022, "ASD Detection Using an Advanced Deep Neural Network," Journal of Information and Optimization Sciences, 43(8), pp. 2143–2152.
[21] Yuan, Y., Chao, M., and Lo, Y., 2017, "Deep Fully Convolutional Networks With Jaccard Distance," 36(9), pp. 1876–1886.
[22] Liu, L., Tsui, Y. Y., and Mandal, M., 2021, "Skin Lesion Segmentation Using Deep Learning with Auxiliary Task," J Imaging, 7(4), p. 67.
[23] Badrinarayanan, V., Kendall, A., and Cipolla, R., 2017, "SegNet: A Deep Convolutional Encoder-Decoder Architecture for Image Segmentation," IEEE Trans Pattern Anal Mach Intell, 39(12), pp. 2481–2495.
[24] Hwang, Y. N., Seo, M. J., and Kim, S. M., 2021, "A Segmentation of Melanocytic Skin Lesions in Dermoscopic and Standard Images Using a Hybrid Two-Stage Approach," Biomed Res Int, 2021, pp. 1–19.
[25] Schaefer, G., Rajab, M. I., Celebi, M. E., and Iyatomi, H., 2011, "Computerized Medical Imaging and Graphics Colour and Contrast Enhancement for Improved Skin Lesion Segmentation," Computerized Medical Imaging and Graphics, 35(2), pp. 99–104.
[26] Wang, R., Chen, S., Ji, C., and Li, Y., 2022, "Cascaded Context Enhancement Network for Automatic Skin Lesion Segmentation," Expert Syst Appl, 201, p. 117069.
[27] Rehman, M., Ali, M., Obayya, M., Asghar, J., Hussain, L., K. Nour, M., Negm, N., and Mustafa Hilal, A., 2022, "Machine Learning Based Skin Lesion Segmentation Method with Novel Borders and Hair Removal Techniques," PLoS One, 17(11), p. e0275781.
[28] Al-masni, M. A., Al-antari, M. A., Choi, M. T., Han, S. M., and Kim, T. S., 2018, "Skin Lesion Segmentation in Dermoscopy Images via Deep Full Resolution Convolutional Networks," Comput Methods Programs Biomed, 162, pp. 221–231.
[29] Ünver, H. M., and Ayan, E., 2019, "Skin Lesion Segmentation in Dermoscopic Images with Combination of YOLO and GrabCut Algorithm," Diagnostics, 9(3), p. 72.
[30] Goyal, M., Oakley, A., Bansal, P., Dancey, D., and Yap, M. H., 2020, "Skin Lesion Segmentation in Dermoscopic Images With Ensemble Deep Learning Methods," IEEE Access, 8, pp. 4171–4181.
[31] Lameski, J., Jovanov, A., Zdravevski, E., Lameski, P., and Gievska, S., 2019, "Skin Lesion Segmentation with Deep Learning," *IEEE EUROCON 2019 -18th International Conference on Smart Technologies*, IEEE, pp. 1–5.
[32] Khan, M. A., Sharif, M., Akram, T., Damaševičius, R., and Maskeliūnas, R., 2021, "Skin Lesion Segmentation and Multiclass Classification Using Deep Learning Features and Improved Moth Flame Optimization," Diagnostics, 11(5), p. 811.
[33] Mustafa, W. A., and Abdul Kader, M. M. M., 2018, "A Review of Histogram Equalization Techniques in Image Enhancement Application," J Phys Conf Ser, 1019, p. 012026.
[34] Rahman, S., Rahman, M. M., Abdullah-Al-Wadud, M., Al-Quaderi, G. D., and Shoyaib, M., 2016, "An Adaptive Gamma Correction for Image Enhancement," EURASIP J Image Video Process, 2016(1), p. 35.
[35] Chiu, Y.-S., Cheng, F.-C., and Huang, S.-C., 2011, "Efficient Contrast Enhancement Using Adaptive Gamma Correction and Cumulative Intensity Distribution," *2011 IEEE International Conference on Systems, Man, and Cybernetics*, IEEE, pp. 2946–2950.
[36] Rahman, S., Rahman, Md. M., Hussain, K., Khaled, S. M., and Shoyaib, M., 2014, "Image Enhancement in Spatial Domain: A Comprehensive Study," *2014 17th International Conference on Computer and Information Technology (ICCIT)*, IEEE, pp. 368–373.
[37] Lee, T., Ng, V., Gallagher, R., Coldman, A., and McLean, D., 1997, "Dullrazor®: A Software Approach to Hair Removal from Images," Comput Biol Med, 27(6), pp. 533–543.
[38] Zafar, M., Amin, J., Sharif, M., Anjum, M. A., Mallah, G. A., and Kadry, S., 2023, "DeepLabv3+-Based Segmentation and Best Features Selection Using Slime Mould Algorithm for Multi-Class Skin Lesion Classification," Mathematics, 11(2), p. 364.
[39] Xie, F., Yang, J., Liu, J., Jiang, Z., Zheng, Y., and Wang, Y., 2020, "Skin Lesion Segmentation Using High-Resolution Convolutional Neural Network," Comput Methods Programs Biomed, 186, p. 105241.
[40] Louhichi, S., Gzara, M., Abdallah, H. ben, Guo, Y., Ashour, A. S., Smarandache, F., Pereira, P. M. M., Fonseca-Pinto, R., Paiva, R. P., Assuncao, P. A. A., Tavora, L. M. N., Thomaz, L. A., Faria, S. M. M., Alvarez, D., and Iglesias, M., 2018, "K-Means Clustering and Ensemble of Regressions: An Algorithm for the ISIC 2017 Skin Lesion Segmentation Challenge," Biomed Signal Process Control, 10(4), pp. 74–79.
[41] Codella, N., Rotemberg, V., Tschandl, P., Celebi, M. E., Dusza, S., Gutman, D., Helba, B., Kalloo, A., Liopyris, K., Marchetti, M., Kittler, H., and Halpern, A., 2019, "Skin Lesion Analysis Toward Melanoma Detection 2018: A Challenge Hosted by the International Skin Imaging Collaboration (ISIC)," pp. 1–12.

[42] Sultana, N. N., Mandal, B., and Puhan, N. B., 2018, "Deep Residual Network with Regularised Fisher Framework for Detection of Melanoma," IET Computer Vision, 12(8), pp. 1096–1104.
[43] [Khan, M. A., Akram, T., Sharif, M., Shahzad, A., Aurangzeb, K., Alhussein, M., Haider, S. I., and Altamrah, A., 2018, "An Implementation of Normal Distribution Based Segmentation and Entropy Controlled Features Selection for Skin Lesion Detection and Classification," BMC Cancer, 18(1), p. 638.
[44] Bozorgtabar, B., Abedini, M., and Garnavi, R., 2016, "Sparse Coding Based Skin Lesion Segmentation Using Dynamic Rule-Based Refinement," pp. 254–261.
[45] Garcia-Arroyo, J. L., and Garcia-Zapirain, B., 2019, "Segmentation of Skin Lesions in Dermoscopy Images Using Fuzzy Classification of Pixels and Histogram Thresholding," Comput Methods Programs Biomed, 168, pp. 11–19.
[46] Bozorgtabar, B., Sedai, S., Roy, P. K., and Garnavi, R., 2017, "Skin Lesion Segmentation Using Deep Convolution Networks Guided by Local Unsupervised Learning," IBM J Res Dev, 61(4/5), pp. 6:1-6:8.
[47] Moradi, N., and Mahdavi-Amiri, N., 2019, "Kernel Sparse Representation Based Model for Skin Lesions Segmentation and Classification," Comput Methods Programs Biomed, 182, p. 105038.
[48] Emre Celebi, M., Kingravi, H. A., Iyatomi, H., Alp Aslandogan, Y., Stoecker, W. v., Moss, R. H., Malters, J. M., Grichnik, J. M., Marghoob, A. A., Rabinovitz, H. S., and Menzies, S. W., 2008, "Border Detection in Dermoscopy Images Using Statistical Region Merging," Skin Research and Technology, 14(3), pp. 347–353.
[49] Bi, L., Kim, J., Ahn, E., Feng, D., and Fulham, M., 2016, "Automated Skin Lesion Segmentation via Image-Wise Supervised Learning and Multi-Scale Superpixel Based Cellular Automata," *2016 IEEE 13th International Symposium on Biomedical Imaging (ISBI)*, IEEE, pp. 1059–1062.
[50] Ahn, E., Kim, J., Bi, L., Kumar, A., Li, C., Fulham, M., and Feng, D. D., 2017, "Saliency-Based Lesion Segmentation Via Background Detection in Dermoscopic Images," IEEE J Biomed Health Inform, 21(6), pp. 1685–1693.
[51] Barın, S., and Güraksın, G. E., 2022, "An Automatic Skin Lesion Segmentation System with Hybrid FCN-ResAlexNet," Engineering Science and Technology, an International Journal, p. 101174.
[52] Ren, Y., Yu, L., Tian, S., Cheng, J., Guo, Z., and Zhang, Y., 2022, "Serial Attention Network for Skin Lesion Segmentation," J Ambient Intell Humaniz Comput, 13(2), pp. 799–810.
[53] Kawahara, J., and Hamarneh, G., 2019, "Fully Convolutional Neural Networks to Detect Clinical Dermoscopic Features," IEEE J Biomed Health Inform, 23(2), pp. 578–585.
[54] Tong, X., Wei, J., Sun, B., Su, S., Zuo, Z., and Wu, P., 2021, "ASCU-Net: Attention Gate, Spatial and Channel Attention U-Net for Skin Lesion Segmentation," Diagnostics, 11(3), p. 501.
[55] Kaul, C., Manandhar, S., and Pears, N., 2019, "Focusnet: An Attention-Based Fully Convolutional Network for Medical Image Segmentation," *2019 IEEE 16th International Symposium on Biomedical Imaging (ISBI 2019)*, IEEE, pp. 455–458.
[56] Liu, L., Mou, L., Zhu, X. X., and Mandal, M., 2019, "Skin Lesion Segmentation Based on Improved U-Net," *2019 IEEE Canadian Conference of Electrical and Computer Engineering (CCECE)*, IEEE, pp. 1–4.
[57] Lei, B., Xia, Z., Jiang, F., Jiang, X., Ge, Z., Xu, Y., Qin, J., Chen, S., Wang, T., and Wang, S., 2020, "Skin Lesion Segmentation via Generative Adversarial Networks with Dual Discriminators," Med Image Anal, 64, p. 101716.
[58] Nazi, Z. al, and Abir, T. A., 2020, "Automatic Skin Lesion Segmentation and Melanoma Detection: Transfer Learning Approach with U-Net and DCNN-SVM," pp. 371–381.
[59] Shahin, A. H., Amer, K., and Elattar, M. A., 2019, "Deep Convolutional Encoder-Decoders with Aggregated Multi-Resolution Skip Connections for Skin Lesion Segmentation," *2019 IEEE 16th International Symposium on Biomedical Imaging (ISBI 2019)*, IEEE, pp. 451–454.
[60] [Salih, O., and Viriri, S., 2020, "Skin Lesion Segmentation Using Stochastic Region-Merging and Pixel-Based Markov Random Field," Symmetry (Basel), 12(8), p. 1224.
[61] L Dora, S Agrawal, R Panda, A Abraham, Optimal breast cancer classification using Gauss–Newton representation based algorithm, Expert Systems with Applications, 97: 134-145, 2017.
[62] A Abraham, Intelligent systems: Architectures and perspectives, Recent advances in intelligent paradigms and applications, Springer, 1-35, 2003.

Author Biographies

Ranjita Rout, a Ph.D. scholar in the Department of Electronics and Communication Engineering, GIET University, Gunupur, Rayagada, Odisha. She has completed her M. Tech in Electronics and Communication Engineering from BPUT, Odisha. Her area of research is Biomedical Image Processing.

Dr. Priyadarsan Parida, working as Associate Professor in the Department of Electronics and Communication Engineering, GIET University, Gunupur, Rayagada, Odisha. He has completed his Ph.D. in Electronics and Communication Engineering from VSSUT, Burla, Odisha. He has completed his M. Tech in Electronics and Communication Engineering from BPUT, Odisha. His area of research are Image processing, Computer Vision, Biomedical Image Analysis, Intelligent Transportation and Biometrics.

Dr. Sonali Dash, working as Professor in the Department of Computer Science Engineering, Chandigarh University, Chandigarh, Punjab. She has completed her Ph.D. in Electronics and Communication Engineering from VSSUT, Burla, Odisha. Her area of research are Biomedical Signal Processing and Pattern Recognition.